

12

AD-A162 739

AFWAL-TR-85-4121

OVERLOAD EFFECTS IN SUSTAINED  
LOAD CRACK GROWTH IN INCONEL 718



T. Weerasooriya  
T. Nicholas

UNIVERSITY OF DAYTON  
RESEARCH INSTITUTE  
300 COLLEGE PARK DRIVE  
DAYTON OH 45469

NOVEMBER 1985

Interim Report Covering Period January 1985 Through October 1985

APPROVED FOR PUBLIC RELEASE; DISTRIBUTION UNLIMITED

FILE COPY

MATERIALS LABORATORY  
AIR FORCE WRIGHT AERONAUTICAL LABORATORIES  
AIR FORCE SYSTEMS COMMAND  
WRIGHT-PATTERSON AIR FORCE BASE OH 45433

DEC 27 1985

FTIC  
D  
E

6 26 26 - 25

NOTICE

When Government drawings, specifications, or other data are used for any purpose other than in connection with a definitely related Government procurement operation, the United States Government thereby incurs no responsibility nor any obligation whatsoever; and the fact that the government may have formulated, furnished, or in any way supplied the said drawings, specifications, or other data, is not to be regarded by implication or otherwise as in any manner licensing the holder or any other person or corporation, or conveying any rights or permission to manufacture use, or sell any patented invention that may in any way be related thereto.

This report has been reviewed by the Office of Public Affairs (ASD/PA) and is releasable to the National Technical Information Service (NTIS). At NTIS, it will be available to the general public, including foreign nations.

This technical report has been reviewed and is approved for publication.



THEODORE NICHOLAS, Matl's Rsch Engr  
Metals Behavior Branch  
Metals and Ceramics Division  
Materials Laboratory

FOR THE COMMANDER



JOHN P. HENDERSON, Chief  
Metals Behavior Branch  
Metals and Ceramics Division  
Materials Laboratory



ALLAN GUNDERSON, Tech Area Mgr  
Metals Behavior Branch  
Metals and Ceramics Division  
Materials Laboratory

"If your address has changed, if you wish to be removed from our mailing list, or if the addressee is no longer employed by your organization please notify AFWAL/MLLN, W-PAFB, OH 45433 to help us maintain a current mailing list".

Copies of this report should not be returned unless return is required by security considerations, contractual obligations, or notice on a specific document.

**REPORT DOCUMENTATION PAGE**

1a. REPORT SECURITY CLASSIFICATION <b>Unclassified</b>		1b. RESTRICTIVE MARKINGS <b>AD-A162 739</b>			
2a. SECURITY CLASSIFICATION AUTHORITY		3. DISTRIBUTION/AVAILABILITY OF REPORT <b>Approved for public release; distribution unlimited</b>			
2b. DECLASSIFICATION/DOWNGRADING SCHEDULE					
4. PERFORMING ORGANIZATION REPORT NUMBER(S)		5. MONITORING ORGANIZATION REPORT NUMBER(S) <b>AFWAL-TR-85-4121</b>			
6a. NAME OF PERFORMING ORGANIZATION <b>University of Dayton Research Institute</b>	6b. OFFICE SYMBOL <i>(If applicable)</i>	7a. NAME OF MONITORING ORGANIZATION <b>Materials Laboratory (AFWAL/MLLN) Air Force Wright Aeronautical Laboratories</b>			
6c. ADDRESS (City, State and ZIP Code) <b>300 College Park Drive Dayton OH 45469</b>		7b. ADDRESS (City, State and ZIP Code) <b>Wright-Patterson Air Force Base OH 45433</b>			
8a. NAME OF FUNDING/SPONSORING ORGANIZATION	8b. OFFICE SYMBOL <i>(If applicable)</i>	9. PROCUREMENT INSTRUMENT IDENTIFICATION NUMBER <b>AF Contract F33615-84-C-5051</b>			
8c. ADDRESS (City, State and ZIP Code)		10. SOURCE OF FUNDING NOS.			
		PROGRAM ELEMENT NO. <b>61102F</b>	PROJECT NO. <b>2302</b>	TASK NO. <b>P1</b>	WORK UNIT NO. <b>01</b>
11. TITLE <i>(Include Security Classification)</i> <b>Overload Effects In Sustained Load Crack Growth In Inconel 718</b>					
12. PERSONAL AUTHOR(S) <b>T. Weerasooriya* and T. Nicholas**</b>					
13a. TYPE OF REPORT <b>Interim</b>	13b. TIME COVERED FROM <u>1/85</u> TO <u>10/85</u>		14. DATE OF REPORT (Yr., Mo., Day) <b>November 1985</b>		15. PAGE COUNT <b>25</b>
16. SUPPLEMENTARY NOTATION <b>*UDRI **AFWAL/MLLN (+ the square root of m)</b>					
17. COSATI CODES		18. SUBJECT TERMS <i>(Continue on reverse if necessary and identify by block number)</i> <b>crack growth, fatigue, overloads, crack growth retardation, nickel base superalloy, elevated temperature</b>			
19. ABSTRACT <i>(Continue on reverse if necessary and identify by block number)</i> <b>Crack-growth-rate experiments were conducted on CT specimens of Inconel 718 at 649°C. The loading spectrum consisted of a single 1 Hz cycle at R = 0.1 and a hold time. The ratio of the amplitude of the hold time to the maximum amplitude of the fatigue cycle, R<sub>in</sub>, was 1.0, 0.9, 0.8 and 0.5 with hold times from 0 to 200 s. Tests were performed under computer controlled constant K conditions using values of the maximum of the fatigue cycle of 40 and 50 MPa·m<sup>0.5</sup>. Data show that for R<sub>in</sub> = 1.0, a linear summation model works well, while at R<sub>in</sub> = 0.9 there is a measurable retardation effect on the crack growth during the hold time. For values of R<sub>in</sub> less than 0.8, the sustained load crack growth is almost completely retarded. A simple retardation model is proposed which can fit the experimental data and is based on the concept of an overload plastic zone being produced by the fatigue cycles. It is concluded that hold times do not contribute to crack growth in this material unless their amplitude is at or near the maximum amplitude of the adjacent fatigue cycles.</b>					
20. DISTRIBUTION/AVAILABILITY OF ABSTRACT UNCLASSIFIED/UNLIMITED <input type="checkbox"/> SAME AS RPT. <input checked="" type="checkbox"/> DTIC USERS <input type="checkbox"/>			21. ABSTRACT SECURITY CLASSIFICATION <b>Unclassified</b>		
22a. NAME OF RESPONSIBLE INDIVIDUAL <b>Theodore Nicholas</b>			22b. TELEPHONE NUMBER <i>(Include Area Code)</i> <b>(513) 255-2689</b>	22c. OFFICE SYMBOL <b>AFWAL/MLLN</b>	

## FOREWORD

Portions of work were performed under a contract with the Metals Behavior Branch (MLLN) of the Materials Laboratory, USAF Contract Number F33615-84-C-5051, under the administration of Dr Theodore Nicholas. This work was performed at the Materials Laboratory and supported, in part, by in-house Project 2302P102.

Accession For	
100-00001	<input checked="" type="checkbox"/>
100-00002	<input type="checkbox"/>
100-00003	<input type="checkbox"/>
100-00004	
100-00005	
100-00006	
100-00007	
100-00008	
100-00009	
100-00010	
100-00011	
100-00012	
100-00013	
100-00014	
100-00015	
100-00016	
100-00017	
100-00018	
100-00019	
100-00020	
100-00021	
100-00022	
100-00023	
100-00024	
100-00025	
100-00026	
100-00027	
100-00028	
100-00029	
100-00030	
100-00031	
100-00032	
100-00033	
100-00034	
100-00035	
100-00036	
100-00037	
100-00038	
100-00039	
100-00040	
100-00041	
100-00042	
100-00043	
100-00044	
100-00045	
100-00046	
100-00047	
100-00048	
100-00049	
100-00050	
100-00051	
100-00052	
100-00053	
100-00054	
100-00055	
100-00056	
100-00057	
100-00058	
100-00059	
100-00060	
100-00061	
100-00062	
100-00063	
100-00064	
100-00065	
100-00066	
100-00067	
100-00068	
100-00069	
100-00070	
100-00071	
100-00072	
100-00073	
100-00074	
100-00075	
100-00076	
100-00077	
100-00078	
100-00079	
100-00080	
100-00081	
100-00082	
100-00083	
100-00084	
100-00085	
100-00086	
100-00087	
100-00088	
100-00089	
100-00090	
100-00091	
100-00092	
100-00093	
100-00094	
100-00095	
100-00096	
100-00097	
100-00098	
100-00099	
100-00100	
100-00101	
100-00102	
100-00103	
100-00104	
100-00105	
100-00106	
100-00107	
100-00108	
100-00109	
100-00110	
100-00111	
100-00112	
100-00113	
100-00114	
100-00115	
100-00116	
100-00117	
100-00118	
100-00119	
100-00120	
100-00121	
100-00122	
100-00123	
100-00124	
100-00125	
100-00126	
100-00127	
100-00128	
100-00129	
100-00130	
100-00131	
100-00132	
100-00133	
100-00134	
100-00135	
100-00136	
100-00137	
100-00138	
100-00139	
100-00140	
100-00141	
100-00142	
100-00143	
100-00144	
100-00145	
100-00146	
100-00147	
100-00148	
100-00149	
100-00150	
100-00151	
100-00152	
100-00153	
100-00154	
100-00155	
100-00156	
100-00157	
100-00158	
100-00159	
100-00160	
100-00161	
100-00162	
100-00163	
100-00164	
100-00165	
100-00166	
100-00167	
100-00168	
100-00169	
100-00170	
100-00171	
100-00172	
100-00173	
100-00174	
100-00175	
100-00176	
100-00177	
100-00178	
100-00179	
100-00180	
100-00181	
100-00182	
100-00183	
100-00184	
100-00185	
100-00186	
100-00187	
100-00188	
100-00189	
100-00190	
100-00191	
100-00192	
100-00193	
100-00194	
100-00195	
100-00196	
100-00197	
100-00198	
100-00199	
100-00200	
100-00201	
100-00202	
100-00203	
100-00204	
100-00205	
100-00206	
100-00207	
100-00208	
100-00209	
100-00210	
100-00211	
100-00212	
100-00213	
100-00214	
100-00215	
100-00216	
100-00217	
100-00218	
100-00219	
100-00220	
100-00221	
100-00222	
100-00223	
100-00224	
100-00225	
100-00226	
100-00227	
100-00228	
100-00229	
100-00230	
100-00231	
100-00232	
100-00233	
100-00234	
100-00235	
100-00236	
100-00237	
100-00238	
100-00239	
100-00240	
100-00241	
100-00242	
100-00243	
100-00244	
100-00245	
100-00246	
100-00247	
100-00248	
100-00249	
100-00250	
100-00251	
100-00252	
100-00253	
100-00254	
100-00255	
100-00256	
100-00257	
100-00258	
100-00259	
100-00260	
100-00261	
100-00262	
100-00263	
100-00264	
100-00265	
100-00266	
100-00267	
100-00268	
100-00269	
100-00270	
100-00271	
100-00272	
100-00273	
100-00274	
100-00275	
100-00276	
100-00277	
100-00278	
100-00279	
100-00280	
100-00281	
100-00282	
100-00283	
100-00284	
100-00285	
100-00286	
100-00287	
100-00288	
100-00289	
100-00290	
100-00291	
100-00292	
100-00293	
100-00294	
100-00295	
100-00296	
100-00297	
100-00298	
100-00299	
100-00300	
100-00301	
100-00302	
100-00303	
100-00304	
100-00305	
100-00306	
100-00307	
100-00308	
100-00309	
100-00310	
100-00311	
100-00312	
100-00313	
100-00314	
100-00315	
100-00316	
100-00317	
100-00318	
100-00319	
100-00320	
100-00321	
100-00322	
100-00323	
100-00324	
100-00325	
100-00326	
100-00327	
100-00328	
100-00329	
100-00330	
100-00331	
100-00332	
100-00333	
100-00334	
100-00335	
100-00336	
100-00337	
100-00338	
100-00339	
100-00340	
100-00341	
100-00342	
100-00343	
100-00344	
100-00345	
100-00346	
100-00347	
100-00348	
100-00349	
100-00350	
100-00351	
100-00352	
100-00353	
100-00354	
100-00355	
100-00356	
100-00357	
100-00358	
100-00359	
100-00360	
100-00361	
100-00362	
100-00363	
100-00364	
100-00365	
100-00366	
100-00367	
100-00368	
100-00369	
100-00370	
100-00371	
100-00372	
100-00373	
100-00374	
100-00375	
100-00376	
100-00377	
100-00378	
100-00379	
100-00380	
100-00381	
100-00382	
100-00383	
100-00384	
100-00385	
100-00386	
100-00387	
100-00388	
100-00389	
100-00390	
100-00391	
100-00392	
100-00393	
100-00394	
100-00395	
100-00396	
100-00397	
100-00398	
100-00399	
100-00400	
100-00401	
100-00402	
100-00403	
100-00404	
100-00405	
100-00406	
100-00407	
100-00408	
100-00409	
100-00410	
100-00411	
100-00412	
100-00413	
100-00414	
100-00415	
100-00416	
100-00417	
100-00418	
100-00419	
100-00420	
100-00421	
100-00422	
100-00423	
100-00424	
100-00425	
100-00426	
100-00427	
100-00428	
100-00429	
100-00430	
100-00431	
100-00432	
100-00433	
100-00434	
100-00435	
100-00436	
100-00437	
100-00438	
100-00439	
100-00440	
100-00441	
100-00442	
100-00443	
100-00444	
100-00445	
100-00446	
100-00447	
100-00448	
100-00449	
100-00450	
100-00451	
100-00452	
100-00453	
100-00454	
100-00455	
100-00456	
100-00457	
100-00458	
100-00459	
100-00460	
100-00461	
100-00462	
100-00463	
100-00464	
100-00465	
100-00466	
100-00467	
100-00468	
100-00469	
100-00470	
100-00471	
100-00472	
100-00473	
100-00474	
100-00475	
100-00476	
100-00477	
100-00478	
100-00479	
100-00480	
100-00481	
100-00482	
100-00483	
100-00484	
100-00485	
100-00486	
100-00487	
100-00488	
100-00489	
100-00490	
100-00491	
100-00492	
100-00493	
100-00494	
100-00495	
100-00496	
100-00497	
100-00498	
100-00499	
100-00500	
100-00501	
100-00502	
100-00503	
100-00504	
100-00505	
100-00506	
100-00507	
100-00508	
100-00509	
100-00510	
100-00511	
100-00512	
100-00513	
100-00514	
100-00515	
100-00516	
100-00517	
100-00518	
100-00519	
100-00520	
100-00521	
100-00522	
100-00523	
100-00524	
100-00525	
100-00526	

## TABLE OF CONTENTS

<u>SECTION</u>		<u>PAGE</u>
1	INTRODUCTION	1
2	EXPERIMENTS	3
3	EXPERIMENTAL RESULTS	5
4	ANALYTICAL MODEL	7
5	DETERMINATION OF CONSTANTS	10
6	DELAY TIMES	12
7	DISCUSSION AND CONCLUSIONS	13
	REFERENCES	15

## LIST OF ILLUSTRATIONS

<u>FIGURE</u>		<u>PAGE</u>
1	Loading Spectrum Consisting of 1 Hz Fatigue Cycle and Sustained Load.	17
2	Crack Growth Rate Data Plotted Against Total Cycle Time for $K_{max} = 40 \text{ MPa m}^{\frac{1}{2}}$ as a Function of Different R Values. Linear Model Data is Also Given in the Figure.	18
3	Crack Growth Rate Data Plotted Against Total Cycle Time for $K_{max} = 50 \text{ MPa m}^{\frac{1}{2}}$ as a Function of Different R Values. Linear Model Data is Also Given in the Figure.	19
4	Schematic Diagram of the Plastic Zones at the Crack Tip.	20
5	Variation of $K_{eff}/K_s$ as a Function of Normalized Crack Advance from the Crack Tip in the Overload Plastic Zone.	21
6	Calculated Crack Growth for Different Values of $\alpha$ for $K_{max} = 40 \text{ MPa m}^{\frac{1}{2}}$ and $R_{in} = 0.9$ . Data are Also Shown in the Figure.	22
7	Calculated Crack Growth Rate for Different Values of $\alpha$ for $K_{max} = 50 \text{ MPa m}^{\frac{1}{2}}$ and $R_{in} = 0.9$ . Data are Also Shown in the Figure.	23
8	Calculated Crack Growth Rate for Various $\alpha$ for $R_{in} = 0.8$ . Data are Also Shown in the Figure.	24
9	Calculated Crack Advance During Sustained Load After the Application of the Overload as a Function of the Sustained Load Time for $R_{in} = 0.9$ and $K_{max} = 40$ and $50 \text{ MPa m}^{\frac{1}{2}}$ as Predicted From the Retardation Model. Predicted Delay Times ( $t_d$ ) are Also Shown in the Figure.	25

## LIST OF TABLES

### TABLE

1 HEAT TREATMENT FOR ALLOY 718

### PAGE

16

SECTION 1  
INTRODUCTION

The recent introduction of a damage tolerant design requirement for critical structural components in U.S. Air Force gas turbine engines has created a need for accurate crack growth predictions [1]. The Engine Structural Integrity Program (ENSIP) requires that a pre-existing flaw be assumed present in a component and that fracture mechanics analysis and testing demonstrate that such flaw will not grow to a catastrophic size during the lifetime of the engine. To meet this requirement, crack growth rates must be predicted under typical mission spectra. For components such as turbine disks and spacers in advanced fighter or attack aircraft, the loading spectrum will generally consist of large amplitude, low frequency fatigue cycles with interspersed hold times. The hold times have durations of tens of seconds with amplitudes anywhere from the maximum of the fatigue cycles to less than half that amount, depending on the type of aircraft and the mission.

Concurrent with a design philosophy change from low cycle fatigue initiation to a fracture mechanics damage tolerant approach, engine operating temperatures have increased steadily. This has led to the development of higher temperature nickel-base superalloys and a tendency to use these alloys under conditions where time-dependent material behavior becomes important. Thus, the effect of hold times in a design spectrum which results in crack growth during the hold times, has to be considered as part of the life prediction methodology. Although there has been substantial effort devoted to the study of elevated temperature sustained load crack growth in numerous materials [2-6], there has been little

research directed at crack growth under mission spectra, particularly when such spectra involve both sustained loads and fatigue cycles with sustained loads at different levels than the maximum load amplitudes of the fatigue cycles.

In a previous investigation, a linear cumulative damage model was applied for the prediction of crack growth rates under simple spectrum loading consisting of fatigue cycles and hold times [7]. For Inconel 718 at 649°C, a material which exhibits a significant amount of time-dependent behavior, it was found that the linear cumulative damage model worked well when hold times were at the same level as the maximum load of the fatigue cycle. Here, the algebraic summation of the fatigue crack growth rate as determined from constant load amplitude fatigue tests and the sustained load crack growth as determined from constant load crack growth tests provided excellent correlation with experiments where the two types of loading were combined. However, when the sustained load level was dropped to 75 percent of the fatigue maximum, the linear summation model broke down completely. The net growth observed experimentally appeared to be due only to the fatigue cycles, and the linear summation model grossly overpredicted the growth rate under the simple spectrum.

This investigation was undertaken to evaluate the range of validity of a linear summation model and to determine the contribution of hold-time loading in a simple spectrum consisting of combinations of fatigue cycles with hold times of various duration and amplitude. A simple analytical model is developed based on the concept that the sustained load crack growth is retarded by the application of the overload fatigue cycles.

## SECTION 2

### EXPERIMENTS

A series of crack-growth-rate experiments was conducted using the simple load spectrum depicted in Figure 1. The spectrum consists of a single fatigue cycle of frequency 1Hz, load ratio  $R=0.1$  and maximum stress intensity factor  $K_m$  of either 40 or 50 MPa·m $^{1/2}$ . Hold times,  $t_H$ , of durations varying from a few seconds to several hundred seconds were applied at amplitudes given by  $K = R_{in} \cdot K_m$  where  $R_{in}$  is the ratio of the amplitude of the hold-time to the maximum amplitude of the fatigue cycle. Values of  $R_{in}$  of 1.0, 0.9, 0.8 and 0.5 were used which correspond to overload ratios of 1.0, 1.11, 1.25 and 2.0, respectively, where the overload ratio is the ratio of  $K_m$  in the "overload" fatigue cycle to the baseline  $K$  of the hold-time load. All tests were conducted on CT specimens of width  $W = 40$  mm and thickness  $b = 10$  mm under computer controlled constant  $K_m$  conditions. The test procedure is described in detail in Reference 8. Crack lengths were determined from compliance readings taken with the aid of an extensometer during the unloading portion of the fatigue cycle.

The material used in this investigation was Inconel 718 at 649°C having a standard heat treatment given in Table 1. The material is identical to that used in several previous investigations where it has been shown that it exhibits significant amounts of time dependent behavior [7,8]. Several test conditions were evaluated on a single test specimen under constant  $K$  control. For each condition, the crack was grown until it could be unequivocally determined that the crack was growing at a constant rate. This was accomplished by continuously monitoring average growth rate

using a least squares linear regression fit to the crack length versus number of cycles data. When no statistically significant deviation from an average growth rate was obtained from additional applied cycles, the growth rate was defined as reaching a steady state value. This value was used in the plots of cycle block growth rate against total cycle time  $T = t_H + l$  (see Figure 1). In most cases, the total crack extension used to establish a steady state growth rate under a given test condition was less than 1 mm and was typically of the order of 0.5 mm. Thus, over 30 test conditions could be evaluated on a single specimen, making it possible to duplicate and verify the growth rate for any given condition. Growth rates in a single specimen were found to be reproducible to an accuracy of 10 percent under a given load spectrum using  $K$  as the crack growth rate correlating parameter. Both the reproducibility of the data and the achievement of constant growth rates under constant  $K$  conditions demonstrate that  $K$  is an adequate correlating parameter for this material.

### SECTION 3

#### EXPERIMENTAL RESULTS

Crack growth rate per cycle block,  $da/dN$ , was plotted as a function of total cycle time,  $T$ , for the cases of  $K_m = 40$  and  $K_m = 50 \text{ MPa}\cdot\text{m}^{\frac{1}{2}}$  in Figures 2 and 3, respectively. Note that a cycle time of 1 s. corresponds to pure fatigue cycling at 1 Hz with no hold time. The symbols in each figure represent the experimentally determined growth rates under constant  $K$  conditions for various values of  $R_{in}$ . The three solid lines in each figure represent, from top to bottom, the analytical predictions from a linear cumulative damage model for values of  $R_{in}$  of 1.0, 0.9 and 0.8, respectively. The linear model numerically adds the growth rate for a single cycle of 1.0 Hz and the contribution from sustained load crack growth,  $\dot{a} \cdot t_H$ , where  $\dot{a}$  is the growth rate per unit time for the sustained load crack growth at a stress intensity factor value  $K_s$ . Values of  $\dot{a}$  as a function of  $K$  were determined from a parallel investigation using the same batch of material [9]. Several constant load tests were conducted to obtain crack length versus time data which were reduced to a versus  $K$  and fit with a sigmoidal equation to provide numerical values of  $\dot{a}$  for any  $K$  value.

The data in Figures 2 and 3 reconfirm the previous observation that a linear cumulative damage model works well for  $R_{in} = 1.0$ , ie when the hold-time load is at the maximum value of the fatigue cycle. For values of  $R_{in} = 0.9$ , the linear model overpredicts by more than a factor of 2, thus there appears to be some retardation of the sustained load crack growth. For values of  $R_{in} = 0.8$ , there does not appear to be any contribution of the hold-time loading for values of hold times up to 200 s, the maximum

used in this investigation. The linear model grossly overpredicts the growth rate for this case. The same observation can be made for  $R_{in} = 0.5$ . For this latter case, results were obtained only for the first set of experiments where  $K_m = 40 \text{ MPa} \cdot \text{m}^{\frac{1}{2}}$ . There was no reason to repeat these very time consuming experiments for  $K_m = 50 \text{ MPa} \cdot \text{m}^{\frac{1}{2}}$ .

## SECTION 4

### ANALYTICAL MODEL

A simple model is developed to predict the crack growth rates under the simple spectrum of Figure 1. The model uses a linear cumulative damage concept by summing the contributions of the single fatigue cycle and the hold-time load. The fatigue cycle is assumed to retard the sustained load crack growth because the latter occurs within an enlarged or overload plastic zone due to the fatigue cycle. This retardation concept, similar to that used by Wheeler [10], is illustrated schematically in Figure 4. The plastic zones due to the sustained load of stress intensity factor  $K_s$  and the overload fatigue cycle of maximum stress intensity  $K_m$  have radii denoted by  $r_p$  and  $\bar{r}_p$  with  $\bar{r}_p \geq r_p$  since  $K_s/K_m \leq 1$ . If the overload is applied when the crack length is  $a_0$ , the tips of the plastic zones due to the baseline (hold-time) load and fatigue overload are at  $a_1$  and  $a_2$ , respectively. For a crack advance of  $\Delta a$  from  $a_0$ , the crack will be growing in an overload plastic zone until  $\Delta a = a_2 - a_1$ . During this time, the growth rate will be retarded. The amount of retardation can be expressed by an effective value of stress intensity factor,  $K_{eff}$ , which is smaller than the applied  $K$ . Using a single-valued function of  $\dot{a}$  versus  $K$  to represent the sustained load growth rate, a value of  $K_{eff}$  less than the applied  $K$  will result in a lower growth rate. For modeling purpose,  $K_{eff}$  is taken in the form

$$K_{eff} = K_s [1 - \alpha \exp(-\beta \Delta a)] \quad (1)$$

where  $\alpha$  and  $\beta$  are parameters to be determined and  $\Delta a$  is the amount of crack extension after application of the overload. The parameter  $\beta$  is chosen such that  $K_{\text{eff}} \rightarrow K_s$  when  $\Delta a = \bar{r}_p - r_p$ , ie steady state crack growth resumes when the crack has traversed the overload plastic zone. This is accomplished by setting

$$\beta \Delta a = \pi \sqrt{2} \quad (2)$$

when  $\Delta a = \bar{r}_p - r_p$ , resulting in a value of  $K_{\text{eff}}/K$  which is within one percent of unity as shown in Figure 5. The plastic zone sizes are taken to be the plane stress values given by

$$\bar{r}_p = \frac{1}{\pi} \left( \frac{K_m}{\sigma_y} \right)^2 \quad , \quad r_p = \frac{1}{\pi} \left( \frac{K_s}{\sigma_y} \right)^2 \quad (3)$$

where  $\sigma_y$  is the uniaxial tensile yield stress of the material. Combining (2) and (3) provides an expression for  $\beta$ :

$$\beta = \frac{\sqrt{2}\pi^2\sigma_y^2}{K_s^2(\gamma^2-1)} \quad (4)$$

where the overload ratio  $\gamma$  is defined as

$$\gamma = \frac{K_m}{K_s} = \frac{1}{R_{in}} \quad (5)$$

It is important to note that  $\beta$  is fully defined from the test conditions and material properties and cannot be used as an adjustable parameter to fit experimental data. Thus, eq. (1) has only one parameter,  $\alpha$ , which can

be chosen to fit data. Referring to Figure 5, it can be seen that the value of  $\alpha$  determines  $K_{eff}$  immediately after the overload application and, therefore, can be used to model the value of sustained load crack growth rate.

## SECTION 5

### DETERMINATION OF CONSTANTS

Analytical predictions were made using a linear cumulative damage model which incorporates the retarded sustained load crack growth behavior given by eq. (1). Computations of crack extension,  $\Delta a$ , were made by numerical integration of  $da/dt$  using 1 s time increments for  $\Delta t$ . The crack growth rate,  $da/dt$ , is expressed in the form of a modified sigmoidal equation fit to experimental sustained load crack growth data [9]. The stress intensity  $K_s$  in the sigmoidal equation is replaced by  $K_{eff}$  from eq. (1). The only parameter which had to be determined was  $\alpha$  and this was accomplished by trial and error by choosing a range of values for  $\alpha$ . The results of these trials are shown in Figures 6 and 7 for  $K_m = 40$  and  $K_m = 50 \text{ MPa}\cdot\text{m}^{\frac{1}{2}}$ , respectively, and for the case of  $R_{in} = 0.9$ . The plots for  $\alpha = 0$  represent the linear summation model for the case of no retardation. It can be seen that values of  $\alpha = 0.15$  and  $\alpha = 0.27$  fit the experimental data for the two cases very well, respectively. It is noted in both cases that the model overpredicts the growth rates for very short hold times below approximately 10 s.

For the case of  $R_{in} = 0.8$ , there appeared to be almost complete retardation for hold times up to the maximum of 200 s used in the experiments. In this situation,  $\alpha$  could not be determined accurately as can be seen in Figure 8. Complete retardation is equivalent to a zero growth rate which corresponds to a value of  $K_{eff} = K^*$  which is the threshold value of  $K$  in the  $\dot{a}$  versus  $K$  representation of the hold-time data. In our modeling of the data using a modified sigmoidal equation,  $K^* = 24 \text{ MPa}\cdot\text{m}^{\frac{1}{2}}$ . Values of  $\alpha = 0.25$  and  $\alpha = 0.4$  represent complete retardation for the cases

of  $K_m = 40$  and  $K_m = 50 \text{ MPa}\cdot\text{m}^{\frac{1}{2}}$ , respectively. To represent the data in Figure 8, values of 0.246 and 0.392, respectively, were chosen.

Calculations were made of the overload plastic zone size, defined as  $\bar{r}_p - r_p$ , through which distance a crack must grow under sustained load before it returns to its steady state growth rate. For the four cases corresponding to the two values of  $K_m$  and for  $R_{in} = 0.8$  and 0.9 for each case, values of this overload zone size ranged from approximately 0.1 to 0.5 mm. Note in Figures 2 and 3 that all of the experimentally measured growth rates per cycle block were well below these values. Thus, for the simple spectrum used, the sustained load crack growth was always within the overload plastic zone and occurred at a reduced rate due to retardation. In fact most of the sustained load crack growth occurs for small values of  $\Delta a/(\bar{r}_p - r_p)$ , or near the origin of the x-axis shown in Figure 5. For these experimental conditions, the parameter  $\alpha$  is the primary factor governing the growth rate in the analytical model. The parameter  $\beta$ , and the shape of the function  $K_{eff}/K_s$  shown in Figure 5, are of secondary importance for short hold times under approximately 100 s.

## SECTION 6

### DELAY TIMES

In studies of fatigue crack growth retardation due to overloads, the concept of a number of delay cycles is commonly used. Here, we introduce the equivalent concept of a delay time for sustained load crack growth. Figure 9 presents plots of the calculated value of  $\Delta a_s$ , the growth during the sustained portion of the load, as a function of the hold times,  $t_H$ , for the cases where  $R_{in} = 0.9$ . Also shown in dashed lines is the crack extension that would occur if there were no retardation. The delay times, or the net gain in time because of the retarded growth rates, are approximately 200 s. as shown in Figure 9. Delay times of approximately 4000 and 8000 s were calculated for the cases where  $R_{in} = 0.8$  and  $K_m = 40$  and 50 MPa·m $^{1/2}$ , respectively. In a parallel investigation on the same material, delay times of approximately 4000 and 20000 s were experimentally measured for  $R_{in} = 0.83$  and  $R_{in} = 0.67$ , respectively, for similar values of  $K_m$  [9].

## SECTION 7

### DISCUSSION AND CONCLUSIONS

For the simple spectrum consisting of a fatigue cycle and a hold time, for the material used in this investigation, the hold time does not contribute to crack growth except when its amplitude is close to that of the maximum of the fatigue cycle. If the sustained load crack growth is considered to be retarded by the single cycle overload, it appears that overload ratios greater than approximately 1.2 severely retard growth for hold times as long as  $10^3$  s.

A single parameter retardation model for sustained load crack growth combined with a linear summation model which adds cyclic and (retarded) sustained load contributions appears to be adequate for predicting crack growth rates under the simple load spectrum used in this investigation. The model correlated data covering a range in hold times up to 200 s, although the model was slightly conservative for short hold times up to approximately 10 s. It appears that in addition to the retardation of the sustained load crack growth due to a fatigue overload, there is also a slight retardation of the fatigue crack growth due to the sustained load. This latter phenomenon was not modeled in this investigation.

Most of the retardation modeled in these experiments covered short hold times corresponding to small crack extensions compared to the size of the overload plastic zone. Thus, the initial growth rates directly after an overload appear to be modeled well. In spite of the fact that overloads are repetitively applied before the crack has grown even a small distance through the overload plastic zone, a steady state growth rate was achieved in all experiments under constant  $K$  conditions. This provides further

evidence for the use of  $K$  as a correlating parameter for sustained load  
crack growth in this material.

## LIST OF REFERENCES

1. Military Standard: Engine Structural Integrity Program (ENSIP), MIL-STD-1783 (USAF) 30 November 1984.
2. Donath, R. C., Nicholas, T., and Fu, L. S. In Fracture Mechanics: Thirteenth Conference, ASTM STP 743, Richard Roberts, Ed., American Society for Testing and Materials, 1981, pp. 186-206.
3. Bain, K. R. and Pelloux, R. M. in Superalloys 1984: Proceedings of the Fifth International Symposium on Superalloys, Maurice Gell, et al, Eds., The Metallurgical Society of AIME, 1984, pp. 389-396.
4. Sadananda, K. and Shahinian, P., Metallurgical Transactions, Vol. 6A, 1975, pp. 1741-1749.
5. Scarlin, R. B., Materials Science and Engineering, Vol. 30, 1977, pp. 55-62.
6. Shahinian, P. and Sadananda, K. in Superalloys 1984: Proceedings of the Fifth International Symposium on Superalloys, Maurice Gell, et al, Eds., The Metallurgical Society of AIME, 1984, pp. 741-750.
7. Nicholas, T. and Weerasooriya, T. in Fracture Mechanics: Seventeenth Symposium, ASTM STP \_\_\_, American Society for Testing and Materials, 1986, pp. xxx-xxx.
8. Nicholas, T., Weerasooriya, T. and Ashbaugh, N. E. in Fracture Mechanics: Sixteenth Symposium, ASTM STP 868, M. F. Kanninen and A. T. Hopper, Eds., American Society for Testing and Materials, 1985, pp. xxx-xxx.
9. Harms, K. E., "Overload Effects on Sustained Load Crack Growth at Elevated Temperature," M. S. Thesis, Air Force Institute of Technology, Wright-Patterson AFB OH, December 1984.
10. Wheeler, D. E., Journal of Basic Engineering, Vol. 94, 1972, pp. 181-186.

TABLE 1  
HEAT TREATMENT FOR ALLOY 718

- STEP 1: Anneal at 968°C (1775°F) for 1 Hour, Then Air Cool to Temperature
- STEP 2: Age Harden at 718°C (1325°F) for 8 Hours, Then Furnace Cool at 56°C/Hr (100°F/Hr) to 621°C (1150°F)
- STEP 3: Age Harden at 621°C (1150°F) for a Total Aging Time in Step 2 and Step 3 of 18 Hours
- STEP 4: Air Cool to Room Temperature

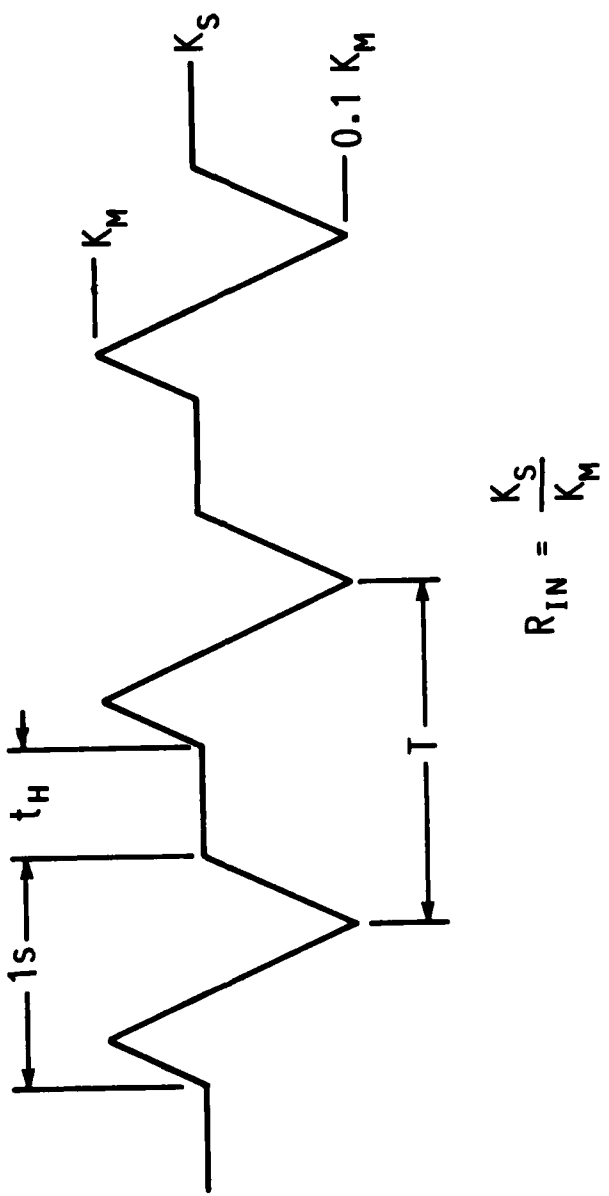


Figure 1. Loading spectrum consisting of 1 Hz fatigue cycle and sustained load.

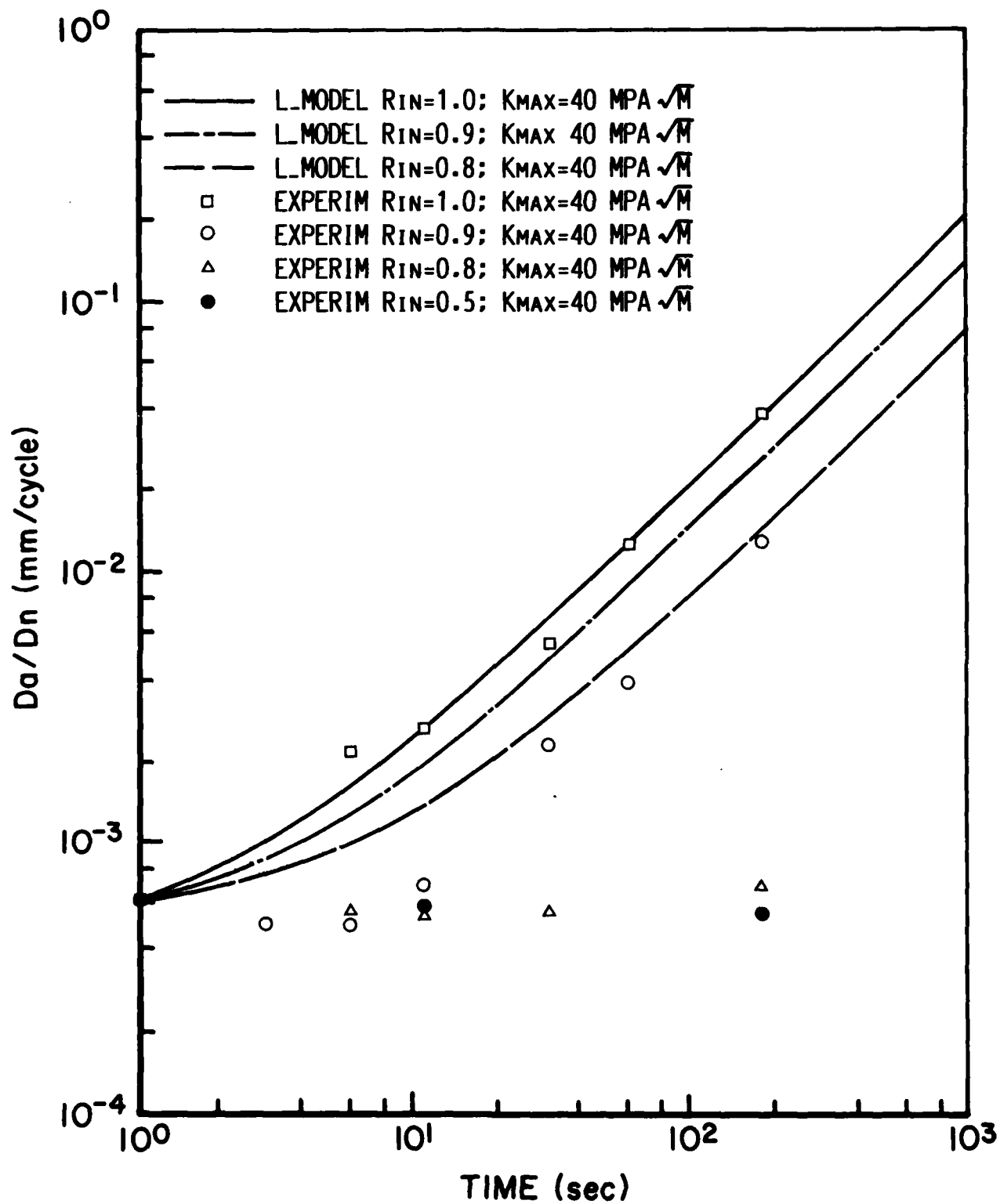


Figure 2. Crack growth rate data plotted against total cycle time for  $K_{max} = 40 \text{ MPa}\cdot\text{m}^{1/2}$  as a function of different  $R_{in}$  values. Linear model data is also given in the figure.

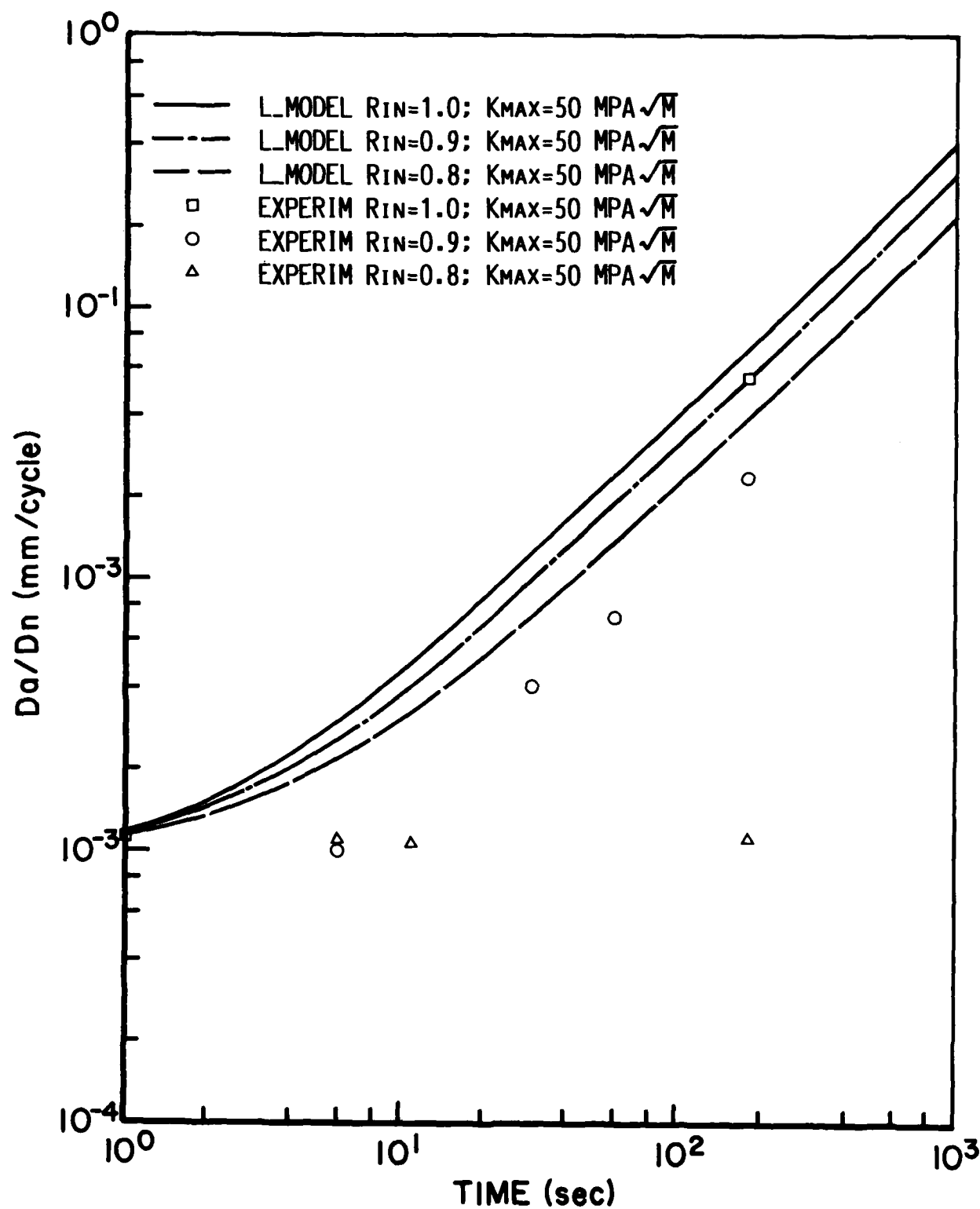


Figure 3. Crack growth rate data plotted against total cycle time for  $K_{MAX} = 50$  MPa $\cdot$ m $^{3/2}$  as a function of different  $R_{IN}$  values. Linear model data is also given in the figure.

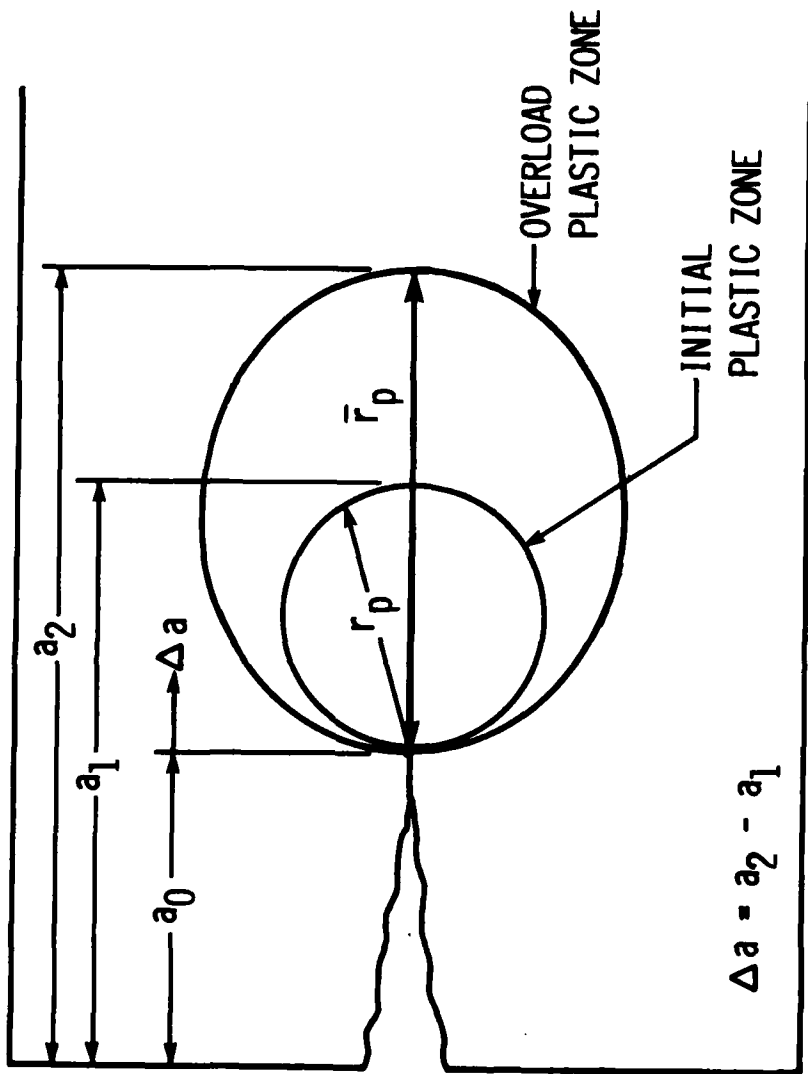


Figure 4. Schematic diagram of the plastic zones at the crack tip.

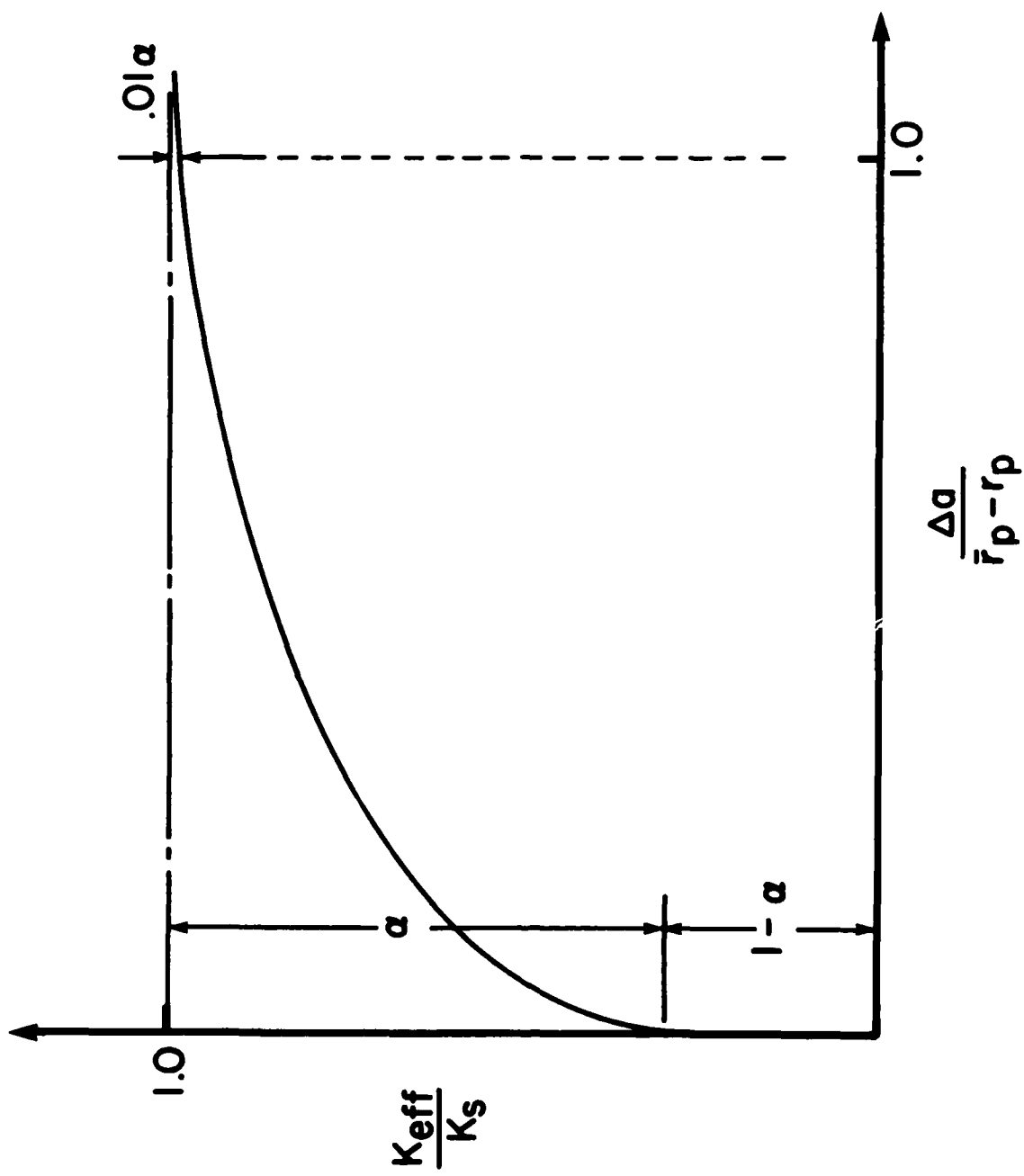


Figure 5. Variation of  $\frac{K_{\text{eff}}}{K_s}$  as function of normalized crack advance from the crack tip in the overload plastic zone.

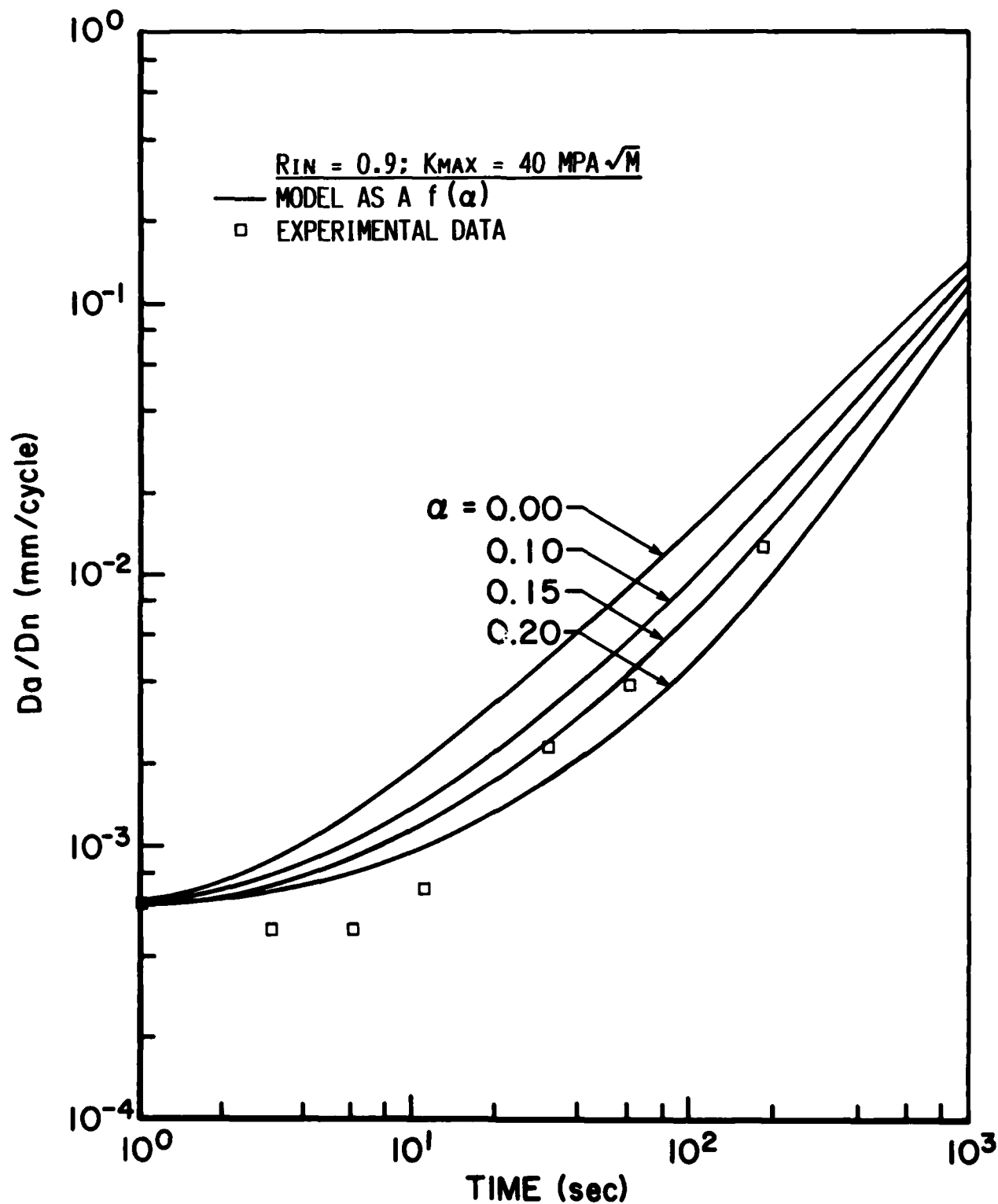


Figure 6. Calculated crack growth for different values of  $\alpha$  for  $K_{max} = 40 \text{ MPa}\cdot\text{m}^{1/2}$  and  $R_{in} = 0.9$ . Data are also shown in the figure.

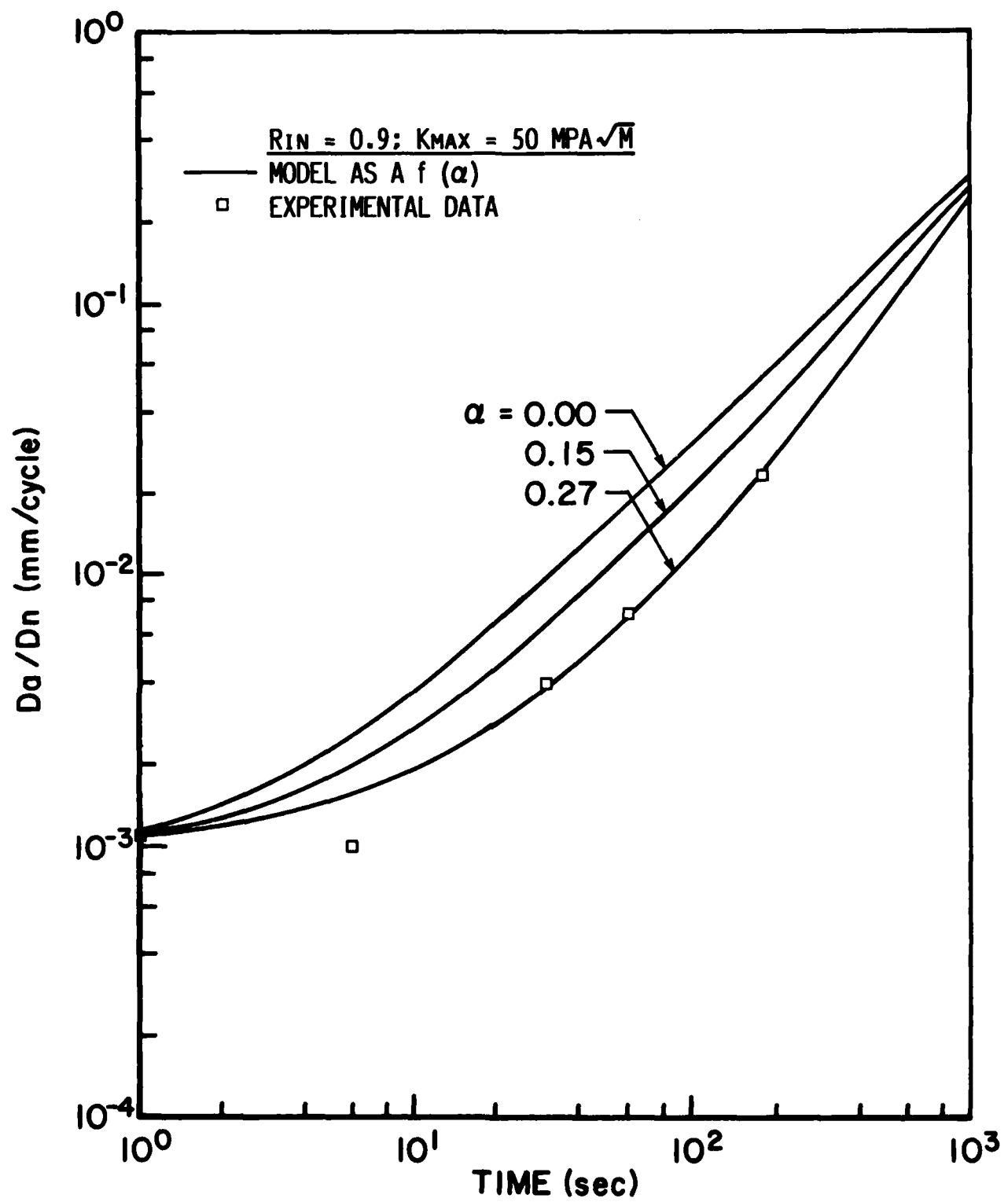


Figure 7. Calculated crack growth rate for different values of  $\alpha$  for  $K_{\max} = 50 \text{ MPa}\cdot\text{m}^{1/2}$  and  $R_{in} = 0.9$ . Data are also shown in the figure.

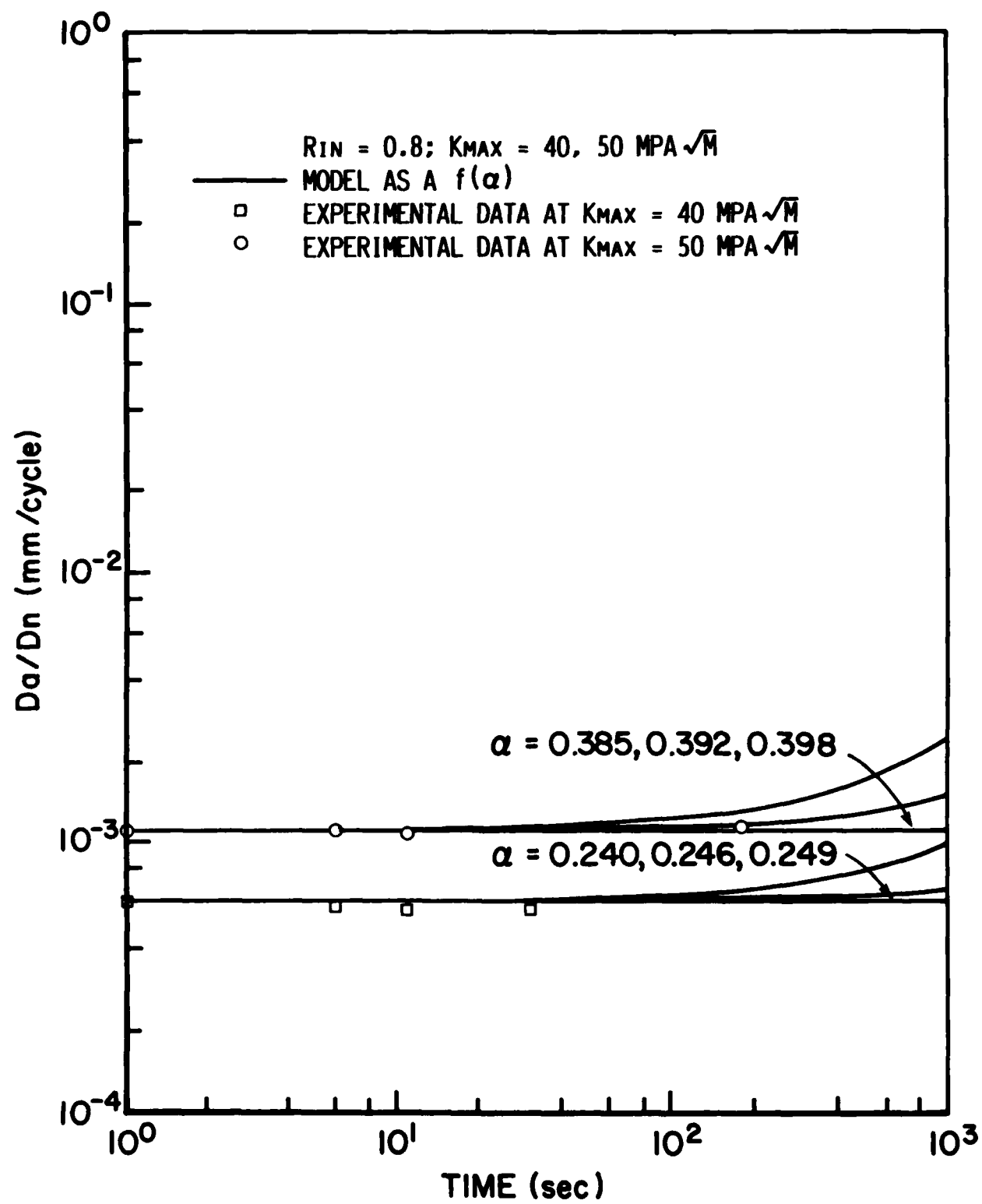


Figure 8. Calculated crack growth rate for various  $\alpha$  for  $R_{in} = 0.8$ . Data are also shown in the figure.

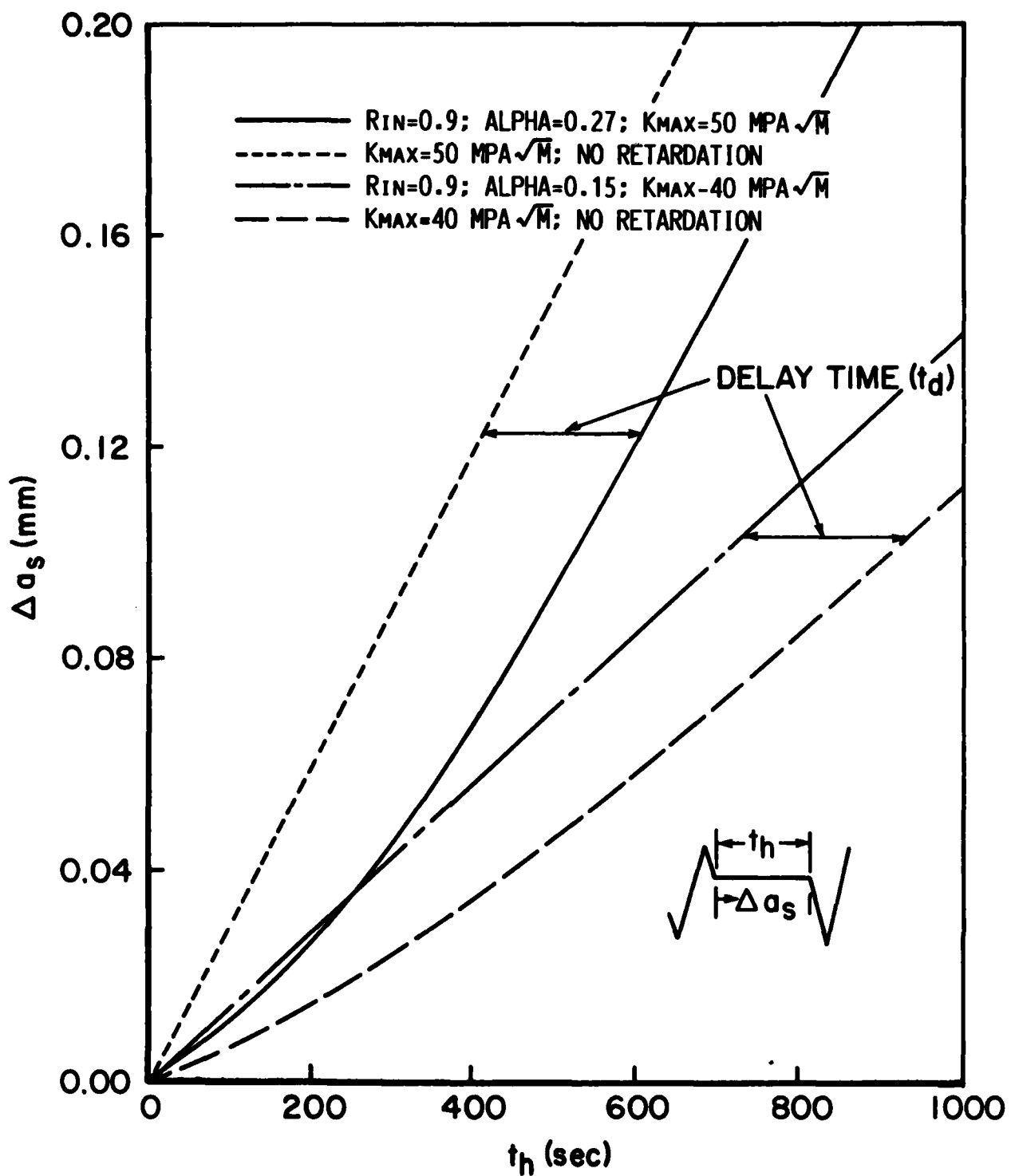


Figure 9. Calculated crack advance during sustained load after the application of the overload as a function of the sustained load time for  $R_{in} = 0.9$  and  $K_{max} = 40$  and  $50 \text{ MPa}\cdot\text{m}^{1/2}$  as predicted from the retardation model. Predicted delay times ( $t_d$ ) are also shown in the figure.